High-frequency electron paramagnetic resonance investigation of the Fe^{3+} impurity center in polycrystalline $PbTiO_3$ in its ferroelectric phase

Hrvoje Meštrić, Rüdiger-A. Eichel,[a] and K.-P. Dinse
Eduard-Zintl-Institute, Darmstadt University of Technology, D-64287 Darmstadt, Germany

Andrew Ozarowski, Johan van Tol, and Louis Claude Brunel
Center for Interdisciplinary Magnetic Resonance, National High Magnetic Field Laboratory, Florida State University, Tallahassee, Florida 32310

(Received 17 June 2004; accepted 31 August 2004)

The intrinsic iron(III) impurity center in polycrystalline lead titanate was investigated by means of high-frequency electron paramagnetic resonance spectroscopy in order to determine the local-environment sensitive fine-structure parameter D. At a spectrometer frequency of 190 GHz, a spectral analysis of a powder sample was unambiguously possible. The observed mean value $D = +35.28$ GHz can be rationalized if Fe^{3+} ions substitute for Ti^{4+} at the B site of the perovskite ABO_3 lattice forming a directly coordinated $Fe'_{Ti}-V_O^{\cdot\cdot}$ defect associate. A consistent fit of the multifrequency data necessitated the use of a distribution of the D values with a variance of about 1 GHz. This statistical distribution of values is probably related to more distant defects and vacancies. © *2004 American Institute of Physics*. [DOI: 10.1063/1.1808477]

I. INTRODUCTION

Lead titanate ($PbTiO_3$, PT) is widely used as a functional ceramic because of its excellent physical and electromechanical properties.[1–4] It is a "displacive-type" ferroelectric material that can be used as a dielectric in capacitors and as a high refractive index thin film for electro-optical components. Its piezoelectric and pyroelectric properties can be utilized in sensors, piezoelectric actuators, and detectors for infrared radiation. As compared to the solid solution system lead zirconate titanate [$Pb(Zr_xTi_{1-x})O_3$, PZT], lead titanate exhibits a higher Curie temperature ($T_C = 763$ K) and a lower dielectric constant of about 200, rendering it more attractive for high-temperature and high-frequency transducer applications.

In order to improve material properties, several transition metals or rare-earth elements may be added on a percentage level, for which reason, considerable interest exists to characterize the role of such extrinsic functional centers. Generally, standard bulk characterization techniques fail due to the inherent low concentration of these centers and electron paramagnetic resonance (EPR) becomes the *method of choice* because of its high sensitivity and selectivity.[5] In particular, if doping with iron is considered, the local symmetry can be explored by monitoring the resulting fine-structure (FS) interaction, which will be modified by the presence of oxygen vacancies ($V_O^{\cdot\cdot}$).[6] If charge compensation occurs in the nearest-neighbor O^{2-}-ion shell, a large distortion of the octahedral symmetry results and because of the short distance, a large change of the intrinsic Fe^{3+} FS tensor will be induced.[7]

Unless crystalline samples are available, these tensor elements in general are not directly accessible at X-band (9.4 GHz) frequencies, since the resulting zero-field splitting (ZFS) is much larger than the microwave (mw) quantum energy. The FS values therefore have to be deduced from the analysis of second-order line shifts in a fully resolved single-crystal spectrum. If only powder samples are available, high-frequency EPR has to be invoked in order to approach high-field conditions, under which an accurate determination of the principal value D of the FS interaction (including sign) via first-order effects is possible.

Beyond its technical importance, we can use lead titanate as a model system related to the considerably more complex acceptor-doped PZT system,[8] because its structure is comparatively simple and well defined. Furthermore, a prerequisite for an analysis of the EPR spectra of solid-solution PZT systems with varying Pb/Zr composition is a complete characterization of the spectra of pure compounds. As stated above, in general, it is quite difficult to extract large ZFS tensor elements from the X-band EPR powder spectra. In order to establish high-frequency EPR as a reliable tool for the investigation of technologically relevant polycrystalline compounds, we have chosen the ubiquitous Fe^{3+} impurity center in lead titanate powder as the first example, because the FS parameters have been obtained by previous single-crystal studies, which can be used for comparison.

The first EPR spectrum, attributed to Fe^{3+} in $PbTiO_3$, led to the discovery of an unusual high FS splitting.[9] This observation was related to the strong tetragonal ferroelectric distortion of the crystalline field. At Q-band (35 GHz), two different iron centers were observed, one of them being assigned to a partially charge-compensated $Fe'_{Ti}-V_O^{\cdot\cdot}$ defect associate. It was also observed that the FS interaction increases by 20% when cooling from room temperature to 77 K, consistent with a change in the lattice deformation, the c/a ratio changing by 19% in this temperature range. The spectra allowed also for the determination of additional terms attributed to higher-rank tensor elements. The temperature dependence of the line intensities at liquid-helium tem-

[a]Author to whom correspondence should be addressed; FAX: +49-6151-16 43 47; electronic mail: eichel@chemie.tu-darmstadt.de

peratures indicated that the sign of D is positive.[10] At 70 GHz, additional transitions could be observed and allowed to refine the ZFS parameters.[11] In contrast to these findings, in a recent X-band EPR study, only a single Fe^{3+} center was observed, for which charge compensation was assumed to occur at distant spheres.[12] This discrepancy was attributed to the different synthesis techniques involved in manufacturing the crystals. Additionally, at low temperatures, a hyperfine structure, assigned to the interaction with the nearby ^{207}Pb nuclei, was observed.

The reported ZFS parameters are spread over a broad range. Since many attempts for gaining structural information about the dopant site, such as the assignment to either $Fe'_{Ti}-V_O^{\cdot\cdot}$ defect associates or noncoordinated "free" Fe'_{Ti} centers with or without off-center shifts of the iron ion, are based upon the size and sign of the ZFS parameters, their precise determination is of considerable importance. By taking the reported interval of the ZFS parameters as input parameters for modeling the structure of the iron center, a contradictory variety of proposed structures results, ranging from free Fe'_{Ti} centers to $Fe'_{Ti}-V_O^{\cdot\cdot}$ defect associates with the off-center shifts toward or away from the oxygen vacancy. In this work, we hence aim for an unambiguous determination of the ZFS parameter by application of high-frequency EPR up to 190 GHz, thus creating the basis for an accurate modeling of the structure. In the magnetic-field range of 2–8 T used, the electron Zeeman energy will be the dominant term in the spin Hamiltonian. The resulting quantization approximately along the field direction significantly simplifies the EPR spectrum. Accordingly, it is possible to accurately determine the ZFS parameters of Fe^{3+} in polycrystalline $PbTiO_3$ from the observed van Hove singularities, which are related to canonical orientations of the compound. High-frequency EPR thus is an indispensable tool for the investigation of technologically relevant PZT, which is commonly available only as a disordered compound.

II. EXPERIMENT

The 9.5-GHz continuous-wave (cw) EPR measurements were performed using an ESP 300E spectrometer (Bruker), equipped with a rectangular TE_{112} resonator. The magnetic field was readout with a NMR Gaussmeter (ER 035M, Bruker) and, as a standard field marker polycrystalline DPPH with $g=2.0036$, was used for the exact determination of the resonance magnetic-field values. The high-frequency EPR measurements were performed at the National High Magnetic Field Laboratory (NHMFL), Tallahassee.[13] The setup used operates in a transmission mode and employs oversized cylindrical waveguides. No resonator was used. Microwave detection was performed with a low-noise, fast-response InSb hot-electron bolometer (QMC Ltd.), operated at liquid-helium temperature. A field modulation in the range of 10–50 kHz was used to obtain "first-derivative-type" EPR spectra.

III. THEORETICAL DESCRIPTION

In principle, a discussion of the Fe^{3+} center in its high-spin form ($S=\frac{5}{2}$) should be based upon the most general form of the spin Hamiltonian, including fourth-rank tensor components.[14] However, literature values of the spin-Hamiltonian parameters for Fe^{3+} ions in lead titanate single crystals, as well as our high-field EPR results justify considerable simplifications. First, since no significant line broadening was observed in the high magnetic fields, the anisotropy of the g matrix apparently imposes much smaller angular-dependent EPR resonance shifts than the inherent peak-to-peak linewidth ΔB_{pp} of the resonance lines and might therefore be neglected. This is in agreement with the expectation because of a vanishing orbital momentum of Fe^{3+} ions. As a consequence, the electron Zeeman interaction will be represented by an isotropic g value. Second, due to the relatively low natural abundance of the only magnetic active isotope ^{57}Fe, the iron hyperfine interaction will be omitted for spectrum reconstruction. Third, the nuclear Zeeman interaction is ignored as well because it does not contribute to EPR spectral features in the first order. Finally, no influence of fourth-rank tensor elements could be experimentally resolved. Hence, the corresponding terms were neglected.

The resulting simplified effective spin Hamiltonian is given by

$$\mathcal{H} = \mathbf{S} \cdot D \cdot \mathbf{S} + g_{\mathrm{iso}} \beta_e B_0 \cdot \mathbf{S}, \tag{1}$$

in which g_{iso} is the electron g factor and β_e the Bohr magneton. The second term is the electronic Zeeman interaction, and B_0 denotes the external field. The first term describes the second-rank fine-structure interaction. This term is often referred to as the zero-field splitting term because it lifts the degeneracy of energy states independent of the magnetic field. The FS tensor D is symmetric and traceless. Thus, there is always a coordinate system in which the tensor is diagonal with the elements $D_{\parallel}$ and $D_{\perp}$. By convention, $D_{\parallel}$ is taken to be the principal value with the largest absolute magnitude. Hence, for axial symmetry, the fine-structure splitting may be described in terms of a single crystal-field parameter that is commonly defined as $D=\frac{3}{2}D_{\parallel}=3D_{\perp}$. The free Fe^{3+} ion has a $3d^5\ ^6S_{5/2}$ ground state. Under the action of a tetragonal crystalline field, this ground state splits into three twofold degenerate levels [cf. Fig. 1(a)].

In the case of the commonly employed X-band frequencies, the zero-field splitting is much larger than the electron Zeeman energy. All the doublets are well separated and only the transitions within each doublet can be observed. Accordingly, the spectrum then is described by defining a separate *effective* spin Hamiltonian with $S'=\frac{1}{2}$ for each doublet. Because of the orientation-dependent state mixing, the effective g' matrices can exhibit a very large anisotropy, even retaining the assumption that the pure electron Zeeman interaction is isotropic.[15] This situation is schematically represented in Figs. 1(a) and 1(c). At zero field, the spins are quantized along the z axis, forming three groups of doubly degenerate states. After application of a static field along the z axis, the quantization along the crystal z axis is retained, the degeneracy being lifted proportional to B_0. However, due to the zero-field splitting being larger than the mw quantum of energy at X-band, only the transitions between levels degenerate at zero field may be induced, providing such transitions

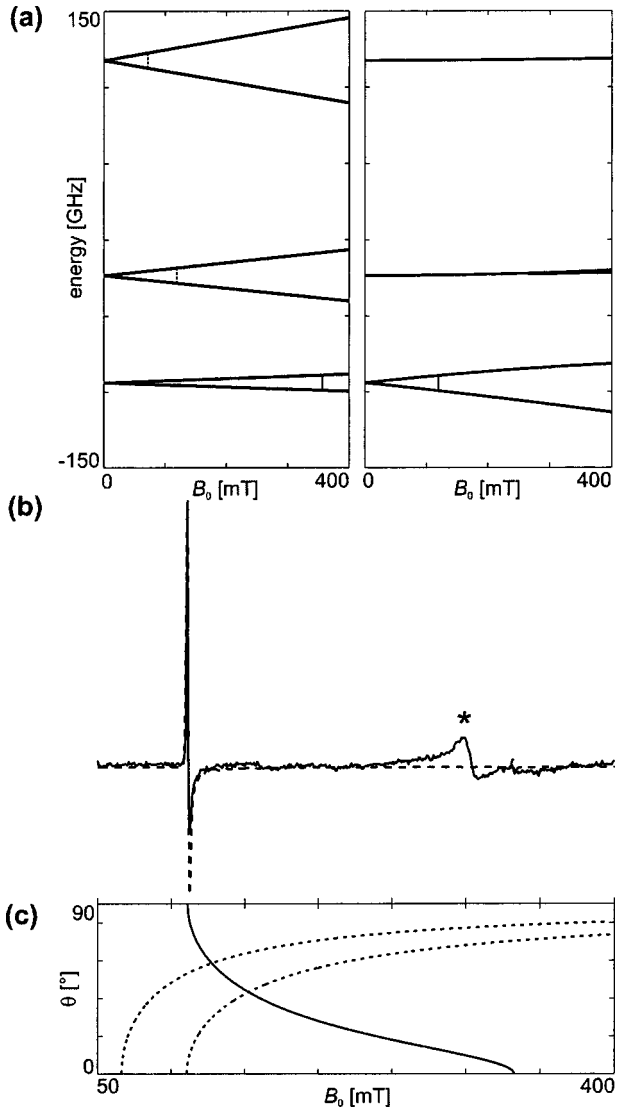

FIG. 1. (a) Schematic representation of the energy levels as a function of the magnetic field for the canonical parallel (left) and perpendicular (right) orientations relative to the ZFS-tensor principal axes for the Fe^{3+} impurity center in $PbTiO_3$. The FS interaction is taken to be positive, $D>0$. The EPR transitions for the *X*-band frequencies are marked by vertical lines involving "allowed" (solid) and "forbidden" transitions (dashed). (b) The *X*-band EPR spectrum (solid) and numerical simulation (dashed) of the Fe^{3+} impurity center in $PbTiO_3$ at $\nu_{mw}=9.320$ GHz and at 10 K. The line at $g=2.2$ marked by an asterisk is tentatively assigned to Pb^{3+} centers. (c) The orientation dependence of the resonance lines for the allowed and forbidden transitions.

are not "forbidden" by the selection rule $\Delta m_S=\pm 1$. If the magnetic field is perpendicular to the *z* axis, there is no first-order splitting of the $|m_S=\pm\frac{5}{2}\rangle$ and $|\pm\frac{3}{2}\rangle$ states, whereas the $|\pm\frac{1}{2}\rangle$ states are split with $g'\approx 6$. Due to the selection rule, all transitions except the $|m_S=+\frac{1}{2}\rangle\leftrightarrow|-\frac{1}{2}\rangle$ transition are forbidden and will not be observed in the *X*-band EPR spectrum.

IV. RESULTS AND DISCUSSION

A typical *X*-band EPR spectrum is presented in Fig. 1(b). It mainly consists of one prominent feature at the low field. In terms of effective *g* values, the spectrum is described with $g'_{\|}=2.004$ and $g'_{\perp}=5.956$. Because all orientations are statistically realized in a powder, the resonances extend from $g'_{\|}$ to $g'_{\perp}$, as illustrated in Fig. 1(c), and because the probability of B_0 being perpendicular to the *z* axis is largest, the resonance peak at $g'_{\perp}$ is the dominant feature. The additional feature at $g=2.2$ can be assigned to the Pb^{3+} centers.[16]

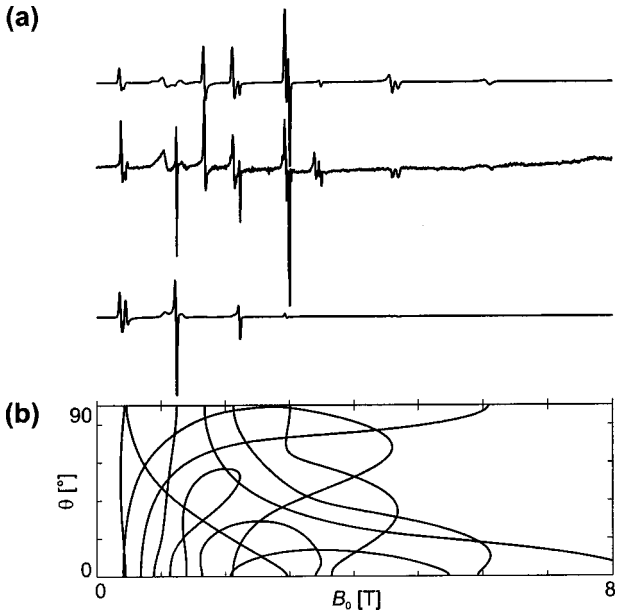

FIG. 2. (a) *W*-band EPR spectrum of the Fe^{3+} impurity center in $PbTiO_3$ at $\nu_{mw}=95.284$ GHz ($T=10$ K). The Numerical spectrum simulations involve B_1 in the perpendicular (top) and parallel (bottom) mode. (b) The orientation dependence of the EPR transitions.

The *W*-band EPR spectrum (95 GHz), depicted in Fig. 2(a), is the representative for an intermediate field regime. For this situation, the crystal-field terms are comparable to the electron Zeeman interaction. Hence, no simple prediction pattern of the EPR spectrum results. The observed sharp lines, however, can be identified as arising from resonances with minor orientation dependence, as shown in Fig. 2(b). To obtain good agreement between the simulation[17] and the experiment, it had to be assumed that the sample was exposed to the oscillating B_1 field components being both parallel and perpendicular to B_0. This phenomenon is caused by multiple reflections and general imperfections (mode impurity) in the mw propagation system, in contrast to cavity-based systems with a well-defined B_1 polarization.[18] For the spectrum simulations, this effect necessitates consideration of parallel and perpendicular EPR modes. In the perpendicular mode, the excitation and detection mw fields are along the laboratory *x* axis, whereas in the parallel mode, they are along the *z* axis, parallel to the external static field. When the magnetic field is parallel to a principal axis, the EPR $\Delta m_S=\pm 2$ transition probability drops to zero with the modulation field B_1 perpendicular to B_0, while it is largest with B_1 parallel to B_0, enabling the observation of forbidden transitions.

At *G* band (190 GHz), EPR is performed almost in the high-field regime. The corresponding energy-level diagrams for the canonical orientation perpendicular relative to the ZFS-tensor principal axes are depicted in Fig. 3(b). The field-energy dependencies are quite complicated because of extensive level mixing, resulting in strongly varying resonance fields for most of the transitions. The EPR spectrum is presented in Fig. 3(a). At low temperatures, the sign of *D* can in principle be determined. This is due to the fact that the

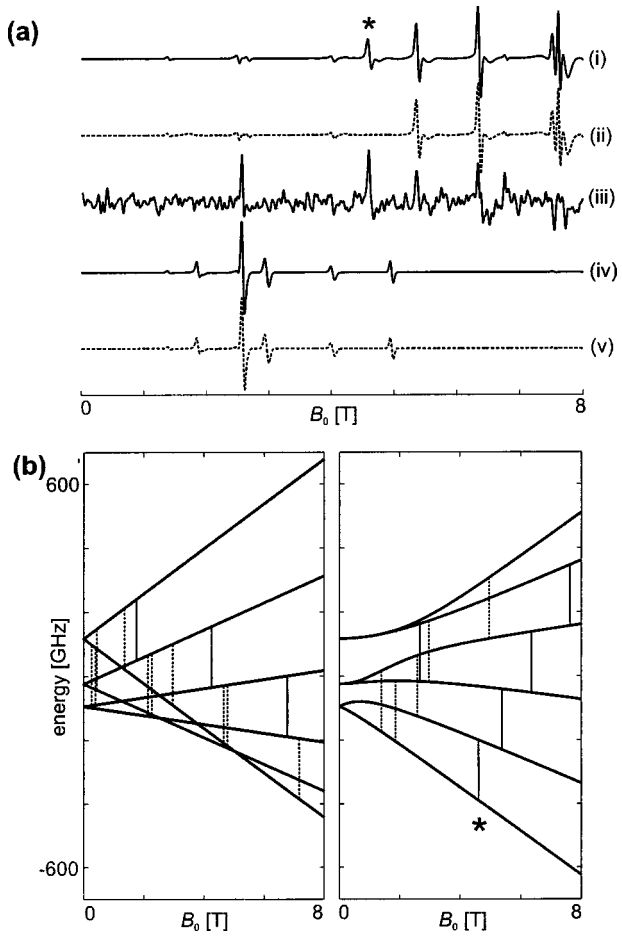

FIG. 3. (a) *G*-band EPR spectrum of the Fe^{3+} impurity center in $PbTiO_3$ at $\nu_{mw}=189.962$ GHz and $T=10$ K (iii). The numerical spectrum simulations involve both B_1 in the perpendicular (i, ii) and parallel (iv, v) mode, as well as a positive (solid) and negative sign (dashed) of the axial ZFS parameter. The transition being particularly sensitive to temperature-dependent level population is marked by an asterisk. (b) The energy levels as a function of the magnetic field for the canonical parallel (left) and perpendicular (right) orientations relative to the ZFS-tensor principal axes using $D>0$. The EPR transitions for *G*-band frequencies are marked by vertical lines involving the allowed (solid) and forbidden transitions (dashed).

transition intensities are a function of the Boltzmann populations of the levels involved. In our case, FS splitting and electron Zeeman energies are much larger than k_BT at 10 K, at which temperature the spectra were recorded for the determination of the sign of *D*. Under these conditions, the temperature dependence of particular resonances allows to determine the sign of the FS parameter *D*. In Fig. 3(a), the results for numerical spectrum simulations assuming a positive (solid) and a negative sign (dashed) of *D* are shown. Because the resonance at 4.61 T (marked by an asterisk) occurs in the calculated spectrum only for $D>0$, the ZFS interaction can be taken as positive. The disappearance of the signal for $D<0$ can be understood by taking into account the calculated energy-level diagrams in Fig. 3(b), where the particular line corresponds to the transition connecting states of the lowest energy. If the sign of *D* would be reversed, this level would be highest in energy and, hence, this transition has to be thermally activated and should be detectable at elevated temperatures only.

The refinement of the spin-Hamiltonian parameters through numerical spectrum simulation simultaneously for all the mw frequencies led to the results summarized in Table I. Using these best-fit values, the numerically simulated spectra are superimposed to the experimental data and show excellent agreement. Concerning the relatively large value of *D*, the local environment for the Fe^{3+} ion can be modeled with the help of the semiempirical *Newman superposition model*.[19] The geometry of the directly coordinated oxygen positions was calculated using the lattice parameters $c=0.422$ nm and $a=0.386$ nm from the x-ray absorption fine-structure measurements at 12 K.[20] The parameters for the iron-oxygen ion pair were taken as $\bar{b}_2=-12.36$ GHz at a reference distance of $R_0=0.2101$ nm and the power-law exponent as $t_2=8$,[21] respectively. Only by assuming that Fe^{3+}, being located at the *B* site, correlated with a directly coordinated oxygen vacancy, the measured value for the ZFS could be reproduced within the centered model.[22] An off-center displacement of the iron in an intact oxygen octahedron leads to a considerably smaller value ($D\leqslant 25$ GHz). Based upon the experimentally determined FS value, the conclusion is thus drawn that iron builds a defect associate with a directly coordinated oxygen vacancy ($Fe'_{Ti}-V_O^{\cdot\cdot}$). These results are in agreement with the predictions obtained by density-functional theory calculations, which are in progress.[23]

Moreover, it can be concluded from the axial symmetry of the ZFS tensor that the orientation of the $Fe'_{Ti}-V_O^{\cdot\cdot}$ defect dipole is along the crystallographic *c* axis. Any other coordi-

TABLE I. *g*-values and FS parameters as obtained from high-field EPR, compared to values from literature with ν_{mw}. The sign of the principal ZFS parameter is determined by an analysis of line intensities at low temperatures. (For a definition of the fourth-order parameters *a* and *F*, see for example, Reference 14.)

Center	g_{iso}	*D* (GHz)	*a* (MHz)	*F* (MHz)	*T* (K)	ν_{mw} (GHz)	
$Fe'-V_O^{\cdot\cdot}$	2.002	35.28±0.01			2–10	9.6–190	This work
Fe'	2.009(5)	27.13±0.01	1678±10	−2833±10	290	9.4	(Ref. 12)
		32±1			77	9.4	
$Fe'-V_O^{\cdot\cdot}$		35.59±0.06	600±210	−510±300	85	70	(Ref. 11)
Fe'		34.48±0.09	660±300	−600±300			
$Fe'-V_O^{\cdot\cdot}$		26.98±1.5			290	37.5	(Ref. 10)
Fe'	2.0	15.89±0.6	809±120				
$Fe'-V_O^{\cdot\cdot}$		32.98±1.5			77		
Fe'	2.0	20.08±0.6					
Fe'	2.009(5)	⩾30				9.4	(Ref. 9)

nation of the oxygen vacancy along either *a* or *b* would reduce the symmetry of the ZFS tensor to orthorhombic, which was not observed within the spectral resolution.

Starting with D as a single fit parameter, a satisfactory reproduction of the experimental data taken at all the different mw frequencies was possible only when allowing for statistical Gaussian distributions δD. Considering the inhomogeneous charge-compensation mechanisms, provided by either the lead vacancies (V''_{Pb}) or valency-altered Pb^{3+} centers, and considering that these defects can be in different shells of the $Fe'_{Ti}-V^{\cdot\cdot}_{O}$ defect associate, a statistical distribution (strain) of the spin-Hamiltonian parameters defined by corresponding variances is expected. In our case, a variance $\delta D = 1$ GHz of the ZFS parameter D, taken to be Gaussian and independent over the mw frequency range from 9.4 to 190 GHz, had to be assumed.

The high-field approach thus allows for determining the absolute value and sign of the axial fine-structure parameter for polycrystalline compounds without ambiguity and even superior accuracy as compared to the single-crystal studies at *X*-band frequencies. This is due to the fact that FS values at high fields can accurately be determined via first-order effects rather than by second-order shifts at low fields. A second consequence is that a distribution δD of the FS parameter is observable as a first-order variation of the line positions that result in a line broadening in the high-field spectra. At *X* band, this effect is of second-order only and, thus, almost vanishes. Hence, no information about D strain can be gathered. In contrast, the fourth-order FS parameters were not accessible by numerical spectrum simulations up to 190 GHz, which in turn are accessible by orientation-dependent single-crystal studies at *X* band.[10–12]

ACKNOWLEDGMENTS

The authors are grateful to Dr. Theo Woike for providing the sample. This research has been financially supported by the DFG priority program 1051 *High-Field EPR in Biology, Chemistry and Physics* and Center of Excellence 595 *Electrical Fatigue in Functional Materials*. The NHMFL is funded by the NSF through Grant No. DMR9016241. One of the authors (K.P.D.) is grateful for a visiting professor fellowship at the NHMFL.

[1]B. Jaffe, W. R. Cook, and H. Jaffe, *Piezoelectric Ceramics* (Academic, London, 1971).
[2]Y. Xu, *Ferroelectric Materials and their Applications* (Elsevier, Amsterdam, 1991).
[3]K. Uchino, *Ferroelectric Devices* (Dekker Inc., New York, 2000).
[4]M. E. Lines and A. M. Glass, *Principles and Applications of Ferroelectrics and Related Materials* (Oxford University Press, Oxford, 2001).
[5]D. Hennings and H. Pomplun, J. Am. Ceram. Soc. **57**, 527 (1974); R. Böttcher, W. Brunner, B. Milsch, G. Völkel, W. Windsch, and S. T. Kirillov, Chem. Phys. Lett. **129**, 546 (1986); R. Heidler, W. Windsch, R. Böttcher, and C. Klimm, Chem. Phys. Lett. **175**, 55 (1990); G. Klotzsche, W. Windsch, and W. Wojcik, Ferroelectr., Lett. Sect. **15**, 115 (1993); O. Bidault, M. Actis, and M. Maglione, Solid State Commun. **95**, 845 (1995); D. J. Keeble, Z. Li, and M. Harmatz, J. Phys. Chem. Solids **57**, 1513 (1996); D. J. Keeble, E. H. Poindexter, and G. J. Gerardi, Appl. Spectrosc. **51**, 117 (1997); W. L. Warren, B. A. Tuttle, B. N. Sun, Y. Huang, and D. A. Payne, Appl. Phys. Lett. **62**, 146 (1993); P. G. Clem, D. A. Payne, and W. L. Warren, J. Appl. Phys. **77**, 5865 (1995); V. V. Laguta, T. V. Antimirova, M. D. Glinchuk, I. P. Bykov, J. Rosa, M. Zaritskii, and L. Jastrabik, J. Phys.: Condens. Matter **9**, 10041 (1997); J. Huang, N. D. Chasteen, and J. J. Fitzgerald, Chem. Mater. **10**, 3848 (1998); K. Hayashi, A. Ando, Y. Hamaji, and Y. Sakabe, Jpn. J. Appl. Phys., Part 1 **37**, 5237 (1998); E. Erdem, R. Böttcher, H. C. Semmelhack, H. J. Glasl, and E. Hartmann, Phys. Status Solidi B **239**, R7 (2003).
[6]The Kröger and Vink notation is used to describe the charge state of the defect with respect to the neutral lattice.
[7]"Intrinsic" in this context refers to the fact that the B-site symmetry in the ferroelectric phase already allows the existence of an axial FS tensor even without the presence of oxygen vacancies.
[8]R.-A. Eichel, H. Kungl, and M. J. Hoffmann, J. Appl. Phys. **95**, 8092 (2004); R.-A. Eichel, K.-P. Dinse, H. Kungl, M. J. Hoffmann, A. Ozarowski, J. van Tol, and L. C. Brunel, Appl. Phys. A: Mater. Sci. Process. (submitted).
[9]D. J. A. Gainon, Phys. Rev. **134**, A1300 (1964).
[10]R. G. Pontin, E. F. Slade, and D. J. E. Ingram, J. Phys. C **2**, 1146 (1969).
[11]O. Lewis and G. Wessel, Phys. Rev. A **13**, 2742 (1976).
[12]V. V. Laguta, M. D. Glinchuk, I. P. Bykov, Y. L. Maksimenko, J. Rosa, and L. Jastrabik, Phys. Rev. B **54**, 12353 (1996).
[13]A. K. Hassan, L. A. Pardi, J. Krzystek, A. Sienkiewicz, P. Goy, M. Rohrer, and L. C. Brunel, J. Magn. Reson. **142**, 300 (2000).
[14]A. Abragam and B. Bleaney, *Electron Paramagnetic Resonance of Transition Ions* (Clarendon, Oxford, 1970).
[15]J. S. Griffith, Biopolymers **1**, 35 (1964); H. H. Wickmann, M. P. Klein, and D. A. Shirley, J. Chem. Phys. **42**, 2113 (1965); W. T. Oosterhuis, Struct. Bonding (Berlin) **20**, 19 (1974); J. R. Pilbrow, J. Magn. Reson. (1969-1992) **31**, 479 (1978).
[16]J. Huang, N. D. Chasteen, and J. J. Fitzgerald, Chem. Mater. **10**, 3848 (1998).
[17]Bruker XSOPHE Simulation Package v.1.1.3; EasySpin MATLAB EPR toolbox v.2.0.3, ETH Zürich.
[18]J. Krzystek, S. A. Zvyagin, A. Ozarowski, A. T. Fiedler, T. C. Brunold, and J. Telser, J. Am. Chem. Soc. **126**, 2148 (2004).
[19]D. J. Newman and B. Ng, Rep. Prog. Phys. **52**, 699 (1989).
[20]N. Sircon, B. Ravel, Y. Yacoby, E. A. Stern, F. Dogan, and J. J. Rehr, Phys. Rev. B **50**, 13168 (1994).
[21]E. Siegel and K. A. Müller, Phys. Rev. B **19**, 109 (1979).
[22]E. Siegel and K. A. Müller, Phys. Rev. B **20**, 3587 (1979).
[23]So. Laubach, St. Laubach, and P. C. Schmidt (private communication).